ISBN: 978-3-95450-247-9 ISSN: 2673-5490 doi: 10.18429/JACoW-IPAC2024-MOPC77

EDDY CURRENT SHIELDING OF THE MAGNETIC FIELD RIPPLE IN THE EIC ELECTRON STORAGE RING VACUUM CHAMBERS*

B. Podobedov†, M. Blaskiewicz, H. Witte,
Brookhaven National Laboratory, Upton, NY, USA

Abstract

The EIC electron storage ring (ESR) has very tight tolerances for the amplitude of electron beam position and size oscillations at the interaction point. The oscillations at the proton betatron frequency and its harmonics are the most dangerous because they could lead to unacceptable proton emittance growth from the oscillating beam-beam kick from the electrons. To estimate the amplitude of these oscillations coming from the magnet power supply current ripple we need to accurately account for the eddy current shielding by the copper vacuum chamber with 4-mm thick wall. At the frequencies of interest, the skin depth is a small fraction of the wall thickness, so the commonly used single-pole expressions for eddy current shielding transfer function do not apply. In this paper we present new (to the best of our knowledge) analytical formulas that adequately describe the shielding for this frequency range and chamber geometry and discuss the implications for the power supply ripple specifications at high frequency.

MOTIVATION

The ESR has very tight tolerances for the beam position and size stability at the interaction point. The oscillations at the proton betatron frequency and harmonics are the most dangerous because they could lead to unacceptable proton emittance growth from the oscillating beam-beam kick from the electrons at the amplitude of the positional oscillations as low as 10^{-4} of the rms beam size [1, 2].

For the ESR revolution frequency f_0=78.2 kHz and the lowest possible value of the fractional part of the betatron tune of ~0.1, these oscillations can be caused by driving sources in the range of ~[8-40] kHz (the frequencies above $f_0/2$ are folded back for once-per-turn beam sampling).

Even at much lower frequencies, down to the single Hz range, the position oscillations at a few percent level of the nominal rms beam size were found to be dangerous [2]. Similarly, present specifications from beam-beam physics call for fractional beam-size stability at low frequencies on the order of 10^{-3} and for much tighter control at some specific higher frequencies, e.g. at twice the betatron frequency [3].

These oscillations can have many different causes including magnet power supply ripple, magnet vibration, noise in the main and crab RF systems, and some collective instabilities. For the magnetic field perturbations originating outside of the vacuum chamber, like the ones due to the current ripple in the magnet power supplies, we need to accurately account for the eddy current shielding by the vacuum chamber.

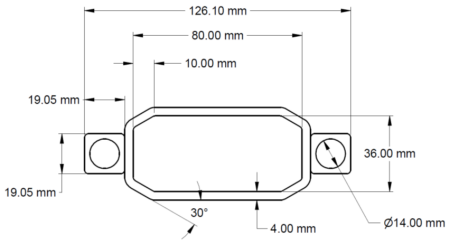

Figure 1: ESR vacuum chamber cross-section.

According to the present design, the dipole and multipole chambers in the ESR have octagonal cross-sections with 4-mm thick copper walls and water-cooling channels on the sides, see Fig. 1. At frequencies above ~300 Hz, the skin depth, δ_{sk}, becomes smaller than the wall thickness. This results in the well-known single-pole expressions for the eddy current shielding (see Eq. (4) below) greatly underestimating the shielding effect at higher frequencies.

In this paper, we present the transfer function (TF) expressions that adequately describe this shielding at any relevant frequency and for magnetic multipoles of arbitrary order. Apart from the shielding, these TFs also describe the phase lag, which is important, for instance, for the fast orbit feedback and other applications.

For simplicity, we first approximate the chamber by an axially symmetric geometry which is sufficient for the power supply ripple specifications at high frequency. Later, we will drop the axial symmetry assumption.

TF FOR THIN-WALL CHAMBERS

Time-varying external magnetic fields are attenuated and delayed inside the vacuum chamber due to the induced eddy currents that flow in the chamber wall. At low frequency, the current variation over the wall thickness due to the skin effect can be neglected (electrically thin wall or weak skin effect approximation). Then, for a non-magnetic beam pipe with a circular cross-section of radius r_0, wall thickness d, and conductivity σ, subjected to a varying external dipole field, $B_e(t) = B_0 \sin(\omega t)$, the field inside is [4, 5]

$$B_i(t) = \frac{B_0}{\sqrt{1+\omega^2\tau^2}} \sin(\omega t - \tan^{-1}(\omega\tau)), \qquad (1)$$

with the time constant given by

$$\tau = \frac{1}{2}\mu_0 \sigma r_0 d, \qquad (2)$$

* Work supported by Brookhaven Science Associates, LLC under Contract No. DE-SC0012704 with the U.S.Department of Energy
† boris@bnl.gov

ISBN: 978-3-95450-247-9 ISSN: 2673-5490 doi: 10.18429/JACoW-IPAC2024-MOPC77

and μ_0 denoting the permeability of free space.

Equation (1) gives the steady-state response of a 1st-order dynamical system with the Laplace-domain ($p = j\omega$) transfer function

$$H_{dipole}(p) = \frac{\tilde{B}_i(p)}{\tilde{B}_e(p)} = \frac{1}{1+p\tau}, \tag{3}$$

which has a single pole at $p = p_0 = -1/\tau$. At frequencies $\omega \gg 1/\tau$ the field attenuation increases by 20 dB/decade and the phase lags the external driving field by $\pi/2$.

Equation (3) can be generalized to higher-order transverse multipole fields (see e.g. [4, 5]). If we use the standard multipole expansion for the vector potential in polar coordinates, i.e. $A_{m,e} = r^m(a_{m,e}\sin m\theta - b_{m,e}\cos m\theta)$, then

$$H_m(p) = \frac{\tilde{a}_{m,i}(p)}{\tilde{a}_{m,e}(p)} = \frac{\tilde{b}_{m,i}(p)}{\tilde{b}_{m,e}(p)} = \frac{1}{1+p\tau/m}, \tag{4}$$

where $\tilde{b}_{m,...}$ and $\tilde{a}_{m,...}$ are the Laplace-transformed regular and skew magnetic multipoles respectively, and the index m=1,2,3,... corresponds to the dipole, quadrupole, sextupole, etc. The e or i index above denotes the external driving field or the field inside the pipe.

Due to the axial symmetry assumed, the TFs for different order multipoles are uncoupled, and the TFs for the regular and skew fields are identical for a given m.

TF FOR ARBITRARY WALL THICKNESS

At higher frequencies, $d \ll \delta_{sk}(\omega)$ no longer applies, so one needs a more general expression for the TF that does not restrict the wall thickness. Such TF can be obtained by standard methods of classical electrodynamics. One can start with the relevant Maxwell's equations in the quasistatic approximation, written in terms of the magnetic vector potential A, select the appropriate multipolar symmetry solutions of the Poisson equation in the interior and exterior regions of the chamber, match the exterior solution to the external field at infinity, and, finally, solve the resulting differential equation for $\tilde{A}$ inside the chamber wall, while matching the boundary conditions. Similar to Eq. (4), the TF is the ratio of the Laplace-transformed multipole inside the pipe to the Laplace-transformed multipole due to the external field alone (i.e. without the pipe). Detailed derivation can be found in [6]. The final result is

$$H_m(p) = \frac{2\,m\left(\frac{b}{a}\right)^m}{a\,b\,q^2(K_{m+1}(a\,q)I_{m-1}(b\,q) - I_{m+1}(a\,q)K_{m-1}(b\,q))}, \tag{5}$$

where $q = (\mu_0\sigma p)^{\frac{1}{2}}$, $a < b$ are the inner and outer chamber radii, and $I_m(...)$ and $K_m(...)$ stand for the modified Bessel functions of order m.

Equivalent expressions to Eq. (5) for the dipole field (m=1) TF can be found in literature, see e.g. [7–10]. However, we are not aware of any published expressions for $m > 1$, so, in this respect, Eq. (5) should be considered new.

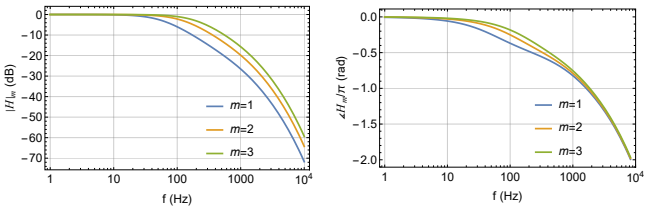

Figure 2: Attenuation (left) and phase lag of the external dipole, quadrupole, and sextupole field inside the beam pipe.

In Fig. 2 we plot the amplitude and phase of the transfer function from Eq. (5) for the three lowest multipoles, using the relevant ESR chamber parameters, i.e. a=18 mm, b=22 mm, and σ=5.8×10^7 $(\Omega \times \mathrm{m})^{-1}$. We took the smallest dimension of the actual chamber cross-section for the radii (the half-height in Fig. 1), so that our shielding estimates remain conservative.

At low frequency, $\delta_{sk} \gg d$, so the TFs seen in Fig. 2 agree with those due to a thin-wall pipe, Eq. (4). This can be also seen directly from Eq. (5), because, in the arguments of the Bessel functions, it holds that $|q| = \sqrt{2}/\delta_{sk}(\omega)$.

However, the high-frequency response in Fig. 2 shows a significant deviation from Eq. (4). The slope of attenuation with frequency keeps increasing beyond 20 dB/decade. The phase lag also increases with accelerating slope, greatly surpassing the $\pi/2$ high-frequency limit of Eq. (4).

To understand this behavior, we can examine the poles of the transfer function given by the roots of the denominator in Eq. (5). From asymptotic properties of the Bessel functions one can establish (see [6] for details) that the dominant pole of the TF is given by

$$p_0 = -m/\tau, \tag{6}$$

where

$$\tau = \frac{1}{2}\mu_0\sigma a d, \tag{7}$$

and small corrections on the order of $O[d/a]$ are omitted. This pole agrees with the one in the thin-wall TF, Eq. (4).

The rest of the poles of Eq. (5) occur at large values of the Bessel function arguments, and they can be approximately expressed as

$$p_n = -n^2\frac{\pi^2}{\mu_0\sigma d^2}, \quad n = 1, 2, 3, ... \tag{8}$$

In contrast to p_0, these poles do not depend on the multipole order m, or the chamber radius, and they scale inversely with the square of the wall thickness.

It is easy to check that these poles correspond to frequencies where $\delta_{sk}(\omega) = \frac{\sqrt{2}}{\pi}\,d/n$. Therefore, when the skin depth is comparable to or smaller than the wall thickness, several of these poles need to be included.

With this understanding of the poles of the transfer function, we suggest a simple rational function approximation,

$$H_m(p) \approx \prod_{n=0}^{N-1}\frac{p_n}{p-p_n}, \tag{9}$$

ISBN: 978-3-95450-247-9 ISSN: 2673-5490 doi: 10.18429/JACoW-IPAC2024-MOPC77

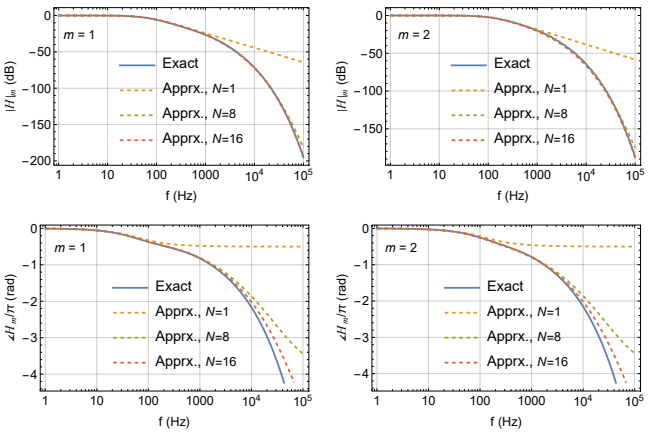

Figure 3: Attenuation (top) and phase lag (bottom) of the external dipole (left) and quadrupole (right) fields inside the beam pipe from Eq. (5) (solid) and Eq. (9) (dashed).

where the poles p_n are given by Eqs. (6)-(8). The total number of poles N should be chosen depending on the highest frequency of interest and the accuracy desired.

For our circular approximation of the ESR chamber cross-section, $|p_0|/2\pi$=60.66 Hz and $|p_{n>0}|/2\pi = n^2 \times 1347$ Hz. Using these values, several dominant pole approximations, together with the exact expression, Eq. (5), are plotted in Fig. 3. The convergence to the exact transfer function with increasing N is evident. Also clear is that the thin-wall approximations, N=1, are only accurate for the attenuation roughly below a kHz, and they greatly underestimate both the attenuation and phase lag at higher frequencies.

Even for an axially symmetric chamber, the field symmetry can be broken due to the boundary conditions at the magnet poles [11]. We confirmed that this results in a lower absolute value of the dominant pole of the TF, i.e. this effect provides additional shielding. Therefore, we have so far disregarded this effect for the sake of conservatism; however, we intend to account for it in the future.

TF FOR ASYMMETRIC CHAMBERS

For axially-asymmetric chambers, the TFs are generally more complicated because all regular and skew multipoles for different m may couple together. Nevertheless, with some further simplifying assumptions, it is possible to extend the approximate TF model, Eq. (9), to axially asymmetric chambers. The idea [12] is to replace the dominant pole p_0 with that found for the thin-wall approximation of the asymmetric chamber while accounting only for the induced currents due to the external field (no self-fields), e.g., for a regular multipole drive, $\tilde{J}_m = \sigma r^m p \tilde{b}_{m,e}(p) \cos m\theta$. Then p_0 can be found from the Biot-Savart law by straightforward integration of $\tilde{J}_m$ over the chamber cross-section.

For the chambers with x and y mid-plane symmetry, the dominant pole of $H_m(p) = \tilde{b}_{m,i}(p)/\tilde{b}_{m,e}(p)$, relating the normal multipoles of the same order, is then

$$p_0^{-1} = -\frac{2^m}{m}\frac{\mu_0 \sigma d}{4\pi}\oint \cos m\theta (\cos\theta)^m \, ds, \qquad (10)$$

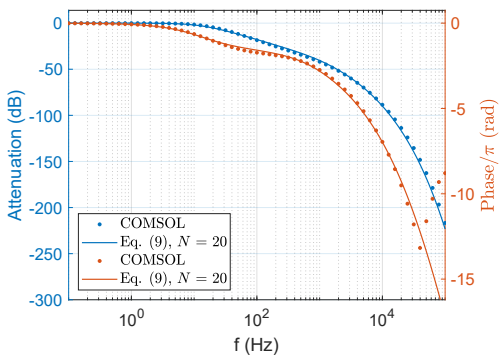

Figure 4: Attenuation and phase lag of the dipole field in the chamber with the cross-section shown in Fig. 1, calculated with COMSOL and from Eqs. (9),(10) and (8).

where $ds = R(\theta)d\theta$. For a circular cross-section chamber, this pole agrees with Eq. (4).

Conversely, the $n > 0$ poles in the TF model given by Eq. (9) can be well-approximated by Eq. (8), derived for an axially-symmetric chamber. This is because the skin effect matters when $\delta_{sk}(\omega) \lesssim d$, so the chamber asymmetries on a spacial scale $\gg d$ do not strongly affect these poles.

The attenuation and phase lag of the external dipole field in the chamber with the cross-section from Fig. 1, calculated with COMSOL [13] and from Eqs. (9),(10), and (8) are plotted in Fig. 4. They show very good agreement except for some artifacts in the COMSOL phase at very high frequency.

CONCLUSION

We derived the transfer function which describes the penetration of time-varying magnetic fields with arbitrary multipole symmetry into a conductive vacuum chamber with a circular cross-section. Our main result, Eq. (5), applies for arbitrary ratios of the skin depth to the wall thickness. We also suggested a simple and physically intuitive approximation of this transfer function, Eq. (9), which is handy for most practical purposes. Finally, we showed how to extend this analytical approach to non-circular chambers and confirmed a good agreement with COMSOL simulations.

The results for the ESR chamber shielding were presented in Figs. 2,3, and 4. The shielding was found to be very strong at high frequencies, e.g. exceeding 70 dB for the dipole above 10 kHz. For the beam position and size oscillations, potentially caused by the magnet power supply ripple at the proton betatron frequency and its harmonics, it is sufficient to take credit just for the chamber shielding, because the resulting PS specifications are not very restrictive [14, 15].

However, at frequencies below approximately 1 kHz, crediting the shielding provided by the chamber alone results in the dipole power supply current ripple specifications at or beyond the state-of-the-art [14]. Therefore, investigating additional sources of shielding and exploring a fast orbit feedback around the interaction point may be necessary to relax the dipole power supply ripple specifications.

ISBN: 978-3-95450-247-9 ISSN: 2673-5490 doi: 10.18429/JACoW-IPAC2024-MOPC77

REFERENCES

[1] M. Blaskiewicz, "Beam-Beam damping of the ion instability", in *Proc. NAPAC'19*, Lansing, MI, USA, Sep. 2019, pp. 391–394. doi:10.18429/JACoW-NAPAC2019-TUPLM11

[2] D. Xu, M. Blaskiewicz, Y. Luo, D. Marx, C. Montag, and B. Podobedov, "Effect of electron orbit ripple on proton emittance growth in EIC", in *Proc. IPAC'23*, Venice, Italy, May 2023, pp. 108–111. doi:10.18429/JACoW-IPAC2023-MOPA039

[3] D. Xu and Y. Luo, private communication, 2024.

[4] R. E. Shafer, "Eddy currents, dispersion relations, and transient effects in superconducting magnets", Fermilab report TM-991, 1980.

[5] D. Rice, "Error sources and effects", in *Handbook of Accelerator Physics and Engineering*, A. W. Chao, M. Tigner, Eds, Singapore, 1998, World Scientific, pp.263-264.

[6] B. Podobedov, M. Blaskiewicz, "Eddy current shielding of the magnetic field ripple in the EIC clectron storage ring vacuum chambers", BNL-224904-2023-TECH, EIC-ADD-TN-055, 2023.

[7] S. Celozzi, R. Araneo, and G. Lovat, *Electromagnetic Shielding*, John Wiley & Sons, Inc., 2008.

[8] S. Fahy, C. Kittel, and S. G. Louie, "Electromagnetic screening by metals", *Am. J. Phys.*, vol. 56, no. 11, pp. 989–992, Nov. 1988. doi:10.1119/1.15353

[9] W. R. Smythe, *Static and Dynamic Electricity*, 3rd ed., Hemisphere Pub. Corp., 1989.

[10] S. H. Kim, "Calculation of pulsed kicker magnetic field attenuation inside beam chambers", APS note LS-291, 2001.

[11] S. Y. Lee, "A multipole expansion for the field of vacuum chamber eddy currents", *Nucl. Instrum. Methods Phys. Res., Sect. A*, vol. 300, no. 1, pp. 151–158, Jan. 1991. doi:10.1016/0168-9002(91)90718-6

[12] B. Podobedov, L. Ecker, D. A. Harder, and G. Rakowsky, "Eddy current shielding by electrically thick vacuum chambers", in *Proc. PAC'09*, Vancouver, Canada, May 2009, paper TH5PFP083, pp. 3398–3400.

[13] https://www.comsol.com/comsol-multiphysics/.

[14] B. Podobedov, M. Blaskiewicz, Y. Luo, D. Marx, C. Montag, and D. Xu, "ESR dipole power supply current ripple and noise specifications", BNL-224464-2023-TECH, EIC-ADD-TN-059, 2023.

[15] B. Podobedov and M. Blaskiewicz, "Transversely driven coherent beam oscillations in the EIC electron storage ring", presented at the IPAC'24, Nashville, TN, USA, May 2024, paper MOPC76, this conference.